Dynamical phase diagram of the two-dimensional p-state clock model

1991 J. Phys. A: Math. Gen. 24 1931

(http://iopscience.iop.org/0305-4470/24/8/031)

J. Phys. A: Math. Gen. 24 (1991) 1931–1945. Printed in the UK

Dynamical phase diagram of the two-dimensional p-state clock model

Y Leroyer† and K Rouidi‡

Laboratoire de Physique Théorique§ Université de Bordeaux I, Rue du Solarium, F-33175 Gradignan Cedex, France

Received 24 September 1990, in final form 7 February 1990

Abstract. We have performed a Monte Carlo study of the dynamical phase diagram of the two-dimensional p-state clock models for $4 \leqslant p \leqslant 10$, by comparing the time evolution of two configurations subjected to the same thermal noise. For $p = 4$, we find the expected two phase structure, similar to the Ising case, with a transition temperature which coincides with the known static one within the error bars. The dynamical critical exponents are measured. For $p \geqslant 5$ we observe, between the low-temperature frozen phase and the high-temperature disordered one, two new phases, which are not present for $p \leqslant 4$. The first is connected to the expected emergence of a spin-wave phase, and the other may be a purely dynamical effect although its connection to the soft phase might suggest the existence of a related equilibrium property. The transition temperatures are determined and are found to satisy a phenomenological duality-like relation.

1. Introduction

The Monte-Carlo dynamics in spin model simulations has been extensively studied, in connection with the static critical properties of the system, principally with a view to improving the performance of the computational method [1]. Recently a new method of investigating the dynamics of spin systems has been proposed [2,3,4]. It is based on the comparison of the time evolution of two initially different configurations subject to the same thermal noise. A distance between the two configurations is defined. From the behaviour of this quantity as a function of the temperature and/or the initial conditions, one can infer information on the dynamical phases of the model. Alternatively, if the starting configurations are very close to each other, one can look for the occurrence of chaotic behaviour, which may simulate the propagation of an original small 'damage' [5].

The two-dimensional Ising model, which was used to test the method in [3], exhibits the expected two-phase structure: a low-temperature phase where the two configurations have a non-zero probability to belong to different valleys in the energy landscape, depending on the initial conditions, and then never meet each other (in the infinite volume limit); a high-temperature phase in which the two configurations meet very

† E-mail address: LEROYER @ FRCPN11 (Bitnet)

‡ Stagiaire de thèse du gouvernement algérien.

§ Unité Associée au CNRS, UA 764.

0305-4470/91/081931+15$03.50

quickly. The transition temperature, determined via finite-size scaling arguments, coincides with the Curie temperature $T_C = 2.269$.

The two-dimensional XY model has been investigated by Golinelli and Derrida [4] who found three different phases: the low-temperature one, where the distance between two configurations after a given time, depends on the initial conditions and is non-zero; an intermediate phase where the distance no longer depends on the initial conditions and but is still non-zero; and a high temperature phase where the two configurations meet very quickly. The transition temperature between the low and intermediate phases is close to the Kosterlitz–Thouless one. The authors of [4] question the origin of the intermediate phase and do not exclude the possibility that it is related to some equilibrium property of the system. Although a more recent result [6] might favour a purely dynamical interpretation of this phase it is of interest to determine which mechanism allows it to exist in the XY model and not in the Ising one.

The Z_p symmetric clock model is defined by the classical Hamiltonian

$$H = -J \sum_{\langle i,j \rangle} \boldsymbol{s}_i \cdot \boldsymbol{s}_j \tag{1}$$

where $\langle i,j \rangle$ runs over the lattice sites and their nearest-neighbours, and J is a positive ferromagnetic coupling. $\boldsymbol{s}_i$ is the unit vector spin at site i whose orientation is quantizesd to the p values

$$\theta_i = n_i \frac{2\pi}{p} \qquad n_i = 0, 1, \ldots, p-1 . \tag{2}$$

In terms of the angular variable θ_i the partition function of the model is

$$Z(\beta) = \sum_{\{\theta_k\}} \exp\left(\beta \sum_{\langle i,j \rangle} \cos(\theta_i - \theta_j)\right) \tag{3}$$

where $\beta = J/T$ (in the following, we set $J = 1$).

This model interpolates between the Ising model ($p = 2$) and the XY model ($p = \infty$). Therefore, investigating the dynamical phase diagrams of these systems as p increases might shed some light on the change of dynamical behaviour and on the connection between dynamical phases and equilibrium properties.

The equilibrium phase diagram of the p-state clock model is rather well known. For $p \leqslant 4$ it has an Ising-like critical behaviour with precisely known exponents and critical temperature [7]. For $p = 5$ one expects the emergence of a soft spin-wave phase between the low-temperature frozen one and the high-temperature disordered one [8,9,10]. As p increases beyond $p = 5$, the lower transition temperature decreases to zero to let only the two-phase (spin-wave, free-vortice) structure survive in the $p = \infty$ limit. The higher transition temperature decreases from $T_c(Z_4) = \frac{1}{2}T_C(\text{Ising}) = 1.135$ to $T_C(Z_\infty) = T_{KT} \simeq 0.9$ [11].

In this paper we have investigated the dynamical phase diagram of the p-state clock models numerically for $p = 4$, 5, 6, 7 and 10 by the method of distances. The technical details are gathered in section 2. In section 3, on the basis of a detailed investigation of the Z_4 and Z_{10} models we relate the different known static phases to the dynamical ones, characterized by the evolution of distances. A dynamic critical exponent is determined from the finite-size scaling analysis of a relaxation time for

the Z_4 model. For the Z_{10} model, an unexpected high-temperature phase occurs above the spin wave phase, extending from $T \simeq 1.0$ up to $T \simeq 2.0$, very similar to the one observed in [4]. Section 4 is devoted to the $Z_{5,6,7}$ models. The same phase structure is observed as in the Z_{10} case, already in the Z_5 model, marking a clear difference with the Ising-like behaviour of the $Z_{2,3,4}$ models. As p increases above 5 this phase structure persists, while the lower transition temperature decreases to zero, as expected. We draw conclusions in the last section, and we propose a duality-like relation between the different transition temperatures.

2. The method

The Z_p clock model (equations (1)–(3)) is simulated on a $L \times L$ lattice ($L = 10, 20$) with periodic boundary conditions by means of the heat bath method. The high-temperature behaviour of this dynamics is identical to the Metropolis one used in [4] as two configurations evolving in the high-temperature phase will eventually meet. This is a necessary condition for a comparison of our results with those of [4]. Furthermore, for our discrete model, the heat bath algorithm is slightly faster, at least for $p \leqslant 10$.

The variable n_i at time t, ($\theta_i = n_i(2\pi/p)$), is updated at time $t + \delta t$ ($\delta t = 1/L^2$), according to the following rule.

(i) for all integers $n \in [0, p-1]$ compute once the probabilities

$$P\{V_i, n\} = \frac{1}{Z\{V_i\}} \exp\left(\frac{J}{T} \sum_{j \in V_i} \cos(n - n_j)\frac{2\pi}{p}\right)$$

where V_i is the set of sites neighbouring the site i, and $Z\{V_i\}$ is such that

$$\sum_{n=0}^{p-1} P\{V_i, n\} = 1$$

and then compute the cumulated probabilities

$$P_0\{V_i\} = 0$$

$$P_k\{V_i\} = \sum_{n=0}^{k-1} P\{V_i, n\} \qquad 1 \leqslant k \leqslant p-1$$

$$P_p\{V_i\} = 1 .$$

(ii) Draw a uniform random number $z \in [0, 1]$. If $P_k \leqslant z < P_{k+1}$ then set the new value of n_i to k.

The dynamics is studied in the following way. Take two different initial configurations $C(0) = \{\theta_i(0)\}$ and $C'(0) = \{\theta'_i(0)\}$ of the system and let them evolve according to the heat bath dynamics, where at each step, the random number z is the same for both configurations. The distance between the two configurations is defined as the generalization of the one used for the Ising model

$$D(t) = \frac{1}{4L^2} \sum_i |s_i - s'_i|^2 \tag{4}$$

$$= \frac{1}{2L^2} \sum_i [1 - \cos(\theta_i(t) - \theta'_i(t))] . \tag{5}$$

This quantity is then suitably averaged over a sample of sequences of random numbers as explained below.

On a finite lattice the probability for two configurations to meet is one in the infinite time limit. Moreover, once the distance is zero it remains zero at any later time. Therefore, if we start with N different initial pair of configurations, the number of pairs which have not yet met at time t (*surviving* configurations) $N_{\text{eff}}(t)$, decreases monotically as the time grows, with a rate dependent on the phase in which the system evolves. Consequently, the value of the distance, averaged over the whole sample, will depend on time. As there is no obvious physical time scale to set a cut-off, we proceed in another way. Actually the time evolution of the *surviving* configurations is very stable in all phases, at least after a thermalization time t_0 which depends on temperature. We therefore compute the averaged distance only over those configurations. As this quantity is rather constant with time it will not depend on the time cut-off $t_{\max}$.

We now define our averaging procedure. We start with a sample of N pairs of initial configurations. We let them evolve with different sequences of random numbers, up to $t = t_{\max}$ where only $N_S = N_{\text{eff}}(t_{\max})$ have survived. If $N_S = 0$ we set $\langle D \rangle = 0$. Otherwise, for each surviving pair we first perform a time average from the thermalization time t_0 up to $t_{\max}$, and then a sampling average over the N_S resulting numbers. The error bars are obtained from the sampling average. This determination of the averaged distance is quite independant of $t_{\max}$ and is very precise in the low-temperature phase, even with samples as small as $N = 20$. In strongly fluctuating phases, we take $N = 100$ to 200, depending on the linear lattice size. We set $t_{\max} = 500$ for the smaller lattices ($L = 10$) and we adjust it by finite-size scaling arguments for the larger ones ($L = 20, 30$—see section 3). This value of $t_{\max}$ is chosen by comparison with another relaxation time which drives the time dependence of the survival probability

$$p_s(t) = \frac{N_{\text{eff}}(t)}{N} . \tag{6}$$

Assuming an exponential-like behaviour

$$p_s(t) = A \exp\left(-\frac{t}{\tau}\right) \tag{7}$$

we determine τ by a two-parameter fit, as a function of the temperature. For our choice, $t_{\max}$ is taken to be order $\tau(T_C)$.

Finally, along with the averaged distance $\langle D \rangle$, we determine the 'susceptibility'

$$\sigma_D(t) = \sqrt{\langle D^2(t) \rangle - \langle D(t) \rangle^2}$$

which measures the fluctuations of $D(t)$ and is very sensitive to the change of phase. The statistical errors on σ_D are estimated from the time average—which gives an underestimation—and by averaging over several sets of random number sequences: we make three to five measurements for some selected temperatures. We shall see in the next sections that the behaviour of all these quantities as functions of the time, temperature and initial conditions provide a set of information sufficient to clearly characterize the different phases of the system.

3. Characterizing the phases

3.1. The Z_4 model

The Z_4 clock model is a special case of the Ashkin–Teller model, and has a second-order phase transition at $T_C(Z_4) = [\ln(\sqrt{2}+1)]^{-1} = 1.135$ [7] separating a low-temperature frozen phase from a high-temperature disordered one, similar to the Ising model. In figure 1 we show the averaged distance $\langle D \rangle$ against the temperature for $L = 10$ and $L = 20$ and for two different initial conditions.

Initialization 1: initial configurations completely polarized in opposite directions $\theta_i(0) = 0$, $\theta'_i(0) = \pi$, $D(0) = 1$.

Initialization 2: initial configurations completely polarized in orthogonal directions $\theta_i(0) = 0$, $\theta'_i(0) = \pi/2$, $D(0) = 0.5$.

For both initializations, we observe an abrupt fall in the region $1.1 \leqslant T \leqslant 1.20$, very close to $T_C = 1.135$. This behaviour is similar to what is observed in the two or three dimensional Ising model [2,3]. It is also in agreement with the picture of valleys in the free energy landscape, which attract the time evolution of the configurations and consequently of the distances between the configurations, depending on the initial conditions. As an illustration of this effect, we show in figure 2 the distribution of the non-zero distances after $t = 500$ for a 10×10 lattice for pairs of configurations initially random and opposite. At $T = 1.0$, the double peak seen in figure 2 clearly shows that after some time the non-zero distances are distributed along the two attractors at $\langle D \rangle = 1$, corresponding $\theta'_i - \theta_i = \pi \; \forall i$, and $\langle D \rangle = 0.5$ corresponding to $\theta'_i - \theta_i = \pi/2 \; \forall i$. For the equivalent distribution at $T = 1.2$ (hatched histogram), in the disordered phase, these attractors have disappeared and the configurations smoothly go to the (always present) $\langle D \rangle = 0$ attractor.

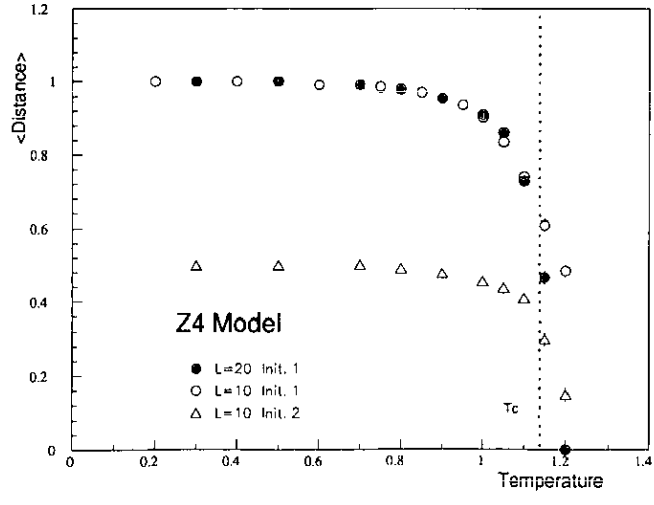

Figure 1. The averaged distance against temperature for the Z_4 model. Open circles, $L = 10$, aligned and opposite initial configurations; open triangles, $L = 10$, aligned and orthogonal initial configurations; full circles, $L = 20$, aligned and opposite initial configurations The dotted line indicates the static critical temperature $T_C = 1.135$.

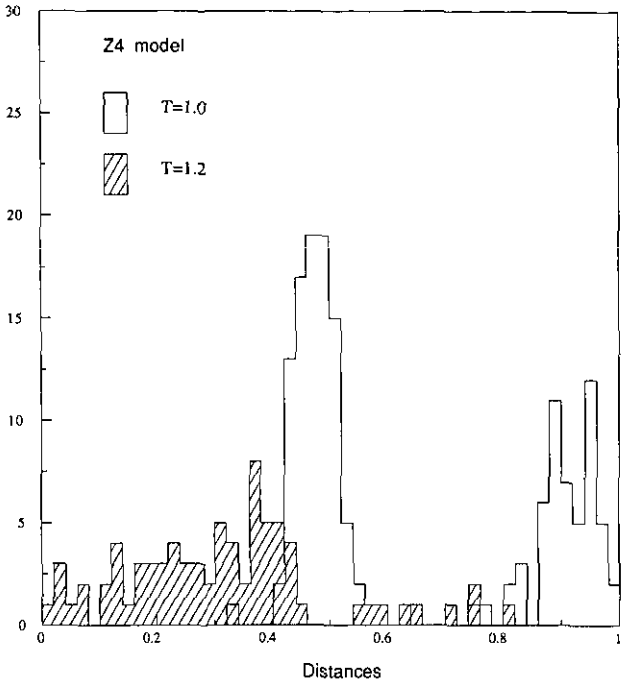

Figure 2. The distribution of distances after t=500 for the Z_4 model on a 10×10 lattice. The hatched histogram corresponds to $T = 1.2$ (symmetric phase) and the other to $T = 1.0$ (broken symmetry phase).

These observations establish a good agreement between the static and the dynamical behaviour and we turn now to more quantitative information. First we notice that a precise determination of the transition temperature is difficult to achieve by using only the averaged distance. In fact, for $T > T_C$, the distances fluctuate strongly and reach zero after a short time; but the average, being taken only over the non-zero distances, remains sizeable. We then decide to set the distance to zero when the number of surviving configurations is less than 10% of the initial sample. This somewhat arbitrary cut-off prevents us from making a precise quantitative determination of the position of the critical temperature and then of the other critical parameters, from the averaged distance only. Therefore we turn to σ_D which measures the fluctuations of $D(t)$ and should be very sensitive to the phase change for the above reasons.

We show the variations of σ_D against the temperature in figure 3 for L=10 and L=20. A sharp peak signals the critical temperature with a rather small finite-size effect. Consequently, in the following, we shall characterize the transition temperature between a ferromagnetic and a disordered phase by the temperature where σ_D exhibits an abrupt jump.

Finally, we determine the dynamic critical exponent of the exponential slope τ of the survival probability, equations (6) and (7). Assuming a finite-size behaviour

$$\tau(T, L) = L^z f(|T - T_C| L^{1/\nu})$$

we have measured $\tau(T = T_C)$ for $L = 10, 15, 20, 30$ for the two initial conditions, initializations 1 and 2 defined above. From the results, displayed in figure 4 we get

$$z = 2.78 \pm 0.11 \qquad \text{for initialization 1}$$

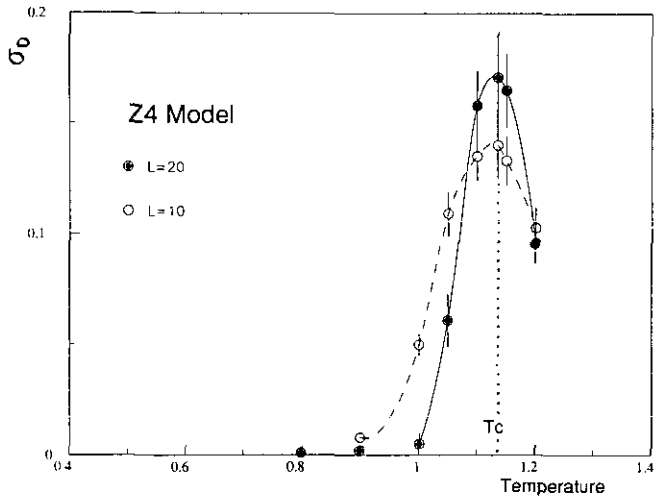

Figure 3. The distance susceptibility σ_D as a function of the temperature for the Z_4 model and $L = 10$ (open circles) and $L = 20$ (full circles). The full and broken lines are guides to the eye. The dotted line indicates the position of T_C.

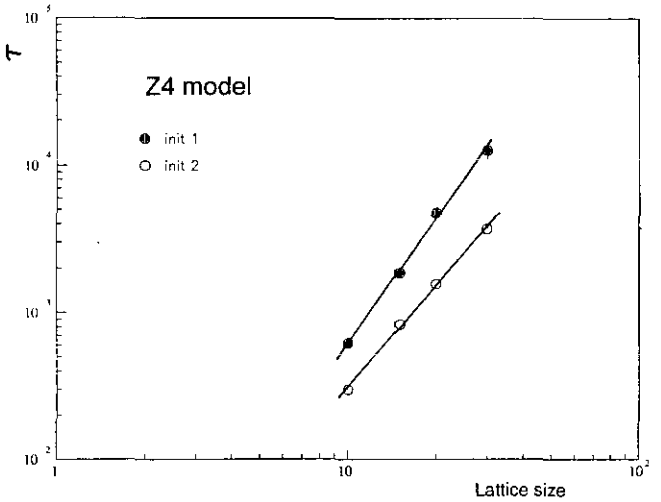

Figure 4. The exponential slope of the survival probability for the Z_4 model at $T = T_C = 1.135$ as a function of the lattice size, for $L = 10, 15, 20, 30$. The full circles correspond to initial configurations aligned and opposite; the open circles to aligned initial configurations but with $\theta_i - \theta_i' = \pi/2$. The straight lines correspond to fitting $\tau \sim L^z$ with $z = 2.29$ (open circles) and $z = 2.78$ (full circles).

$z = 2.29 \pm 0.07$ for initialization 2.

These small errors are only of statistical origin and they presumably underestimate possible corrections to the asymptotic scaling law due to the rather small lattice sizes. However, the value of z for initialization 2 is compatible with that obtained in [3] and this may be an indication for some kind of universality similar to what is found for the Potts model dynamics in [12]. The larger value for the exponent in the case of

initialization 1 may be understood by the fact that configurations leaving the $\langle D \rangle = 1$ attractor have a non-zero probability to fall into the $\langle D \rangle = 0.5$ one, before eventually being trapped in the zero-distance state. Such intermediate attractors, between the fully polarized opposite spin configuration one ($\langle D \rangle = 1$) and the zero-distance one occur in the Z_p models only for $p \geqslant 4$.

3.2. The Z_{10} model

The Z_p model is known to have a Kosterlitz–Thouless (KT) like phase transition for p large enough [13]. This critical behaviour is assumed to be present already in the Z_{10} model which has been investigated in [14]. Three phases are observed: the spin wave phase is found between a low-temperature ferromagnetic one, and a high-temperature symmetric phase. The higher transition temperature is close to that of the XY model ($0.9 \leqslant T \leqslant 1.0$). We now turn to the dynamic behaviour of the model.

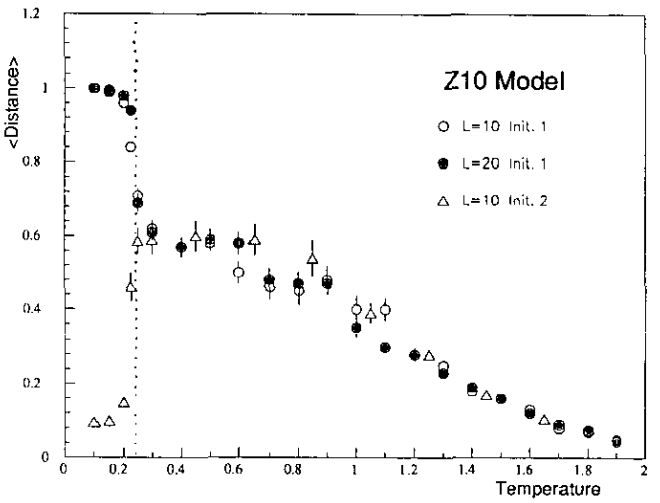

Figure 5. The averaged distance as a function of the temperature for the Z_{10} model. Open and full circles correspond to $L = 10$ and $L = 20$ lattices respectively, and to initial configurations aligned and opposite. The triangles are for an $L = 10$ lattice with initial configurations fully polarized along directions making an angle of $\pi/5$. The dotted line indicates the position of the first transition at $T_1 = 0.24$.

We display in figure 5 the averaged distance as a function of the temperature for the $L = 10$ and $L = 20$ lattices and fully polarized opposite spin initialization (initialization 1). A sharp drop, observed for $T \simeq 0.24$, signals a first transition which is confirmed by the behaviour of σ_D shown in figure 6. However the nature of the high-temperature phase is clearly different from a standard paramagnetic one, as neither $\langle D \rangle$ nor σ_D decreases to zero (see subsection 3.1). The time dependence of the distances in this phase is revealed in figure 7 where we have plotted the time history of a single pair of configurations at $T = 0.25$. As both configurations evolve, their distance jumps from one attractor to another. These attractors correspond to the distance between configurations such that

$$\theta_i' - \theta_i = k\frac{\pi}{5} \qquad \forall i \quad k \in [1,4]$$

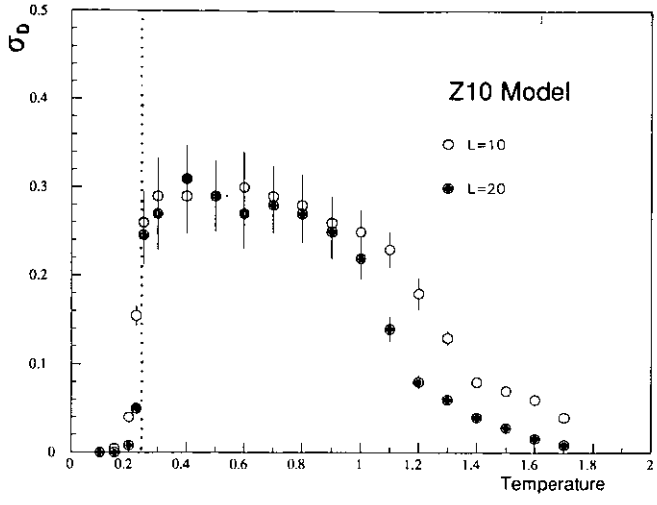

Figure 6. The distance susceptibility σ_D as a function of the temperature for the Z_{10} model for $L = 10$ (open circles) and $L = 20$ (full circles).

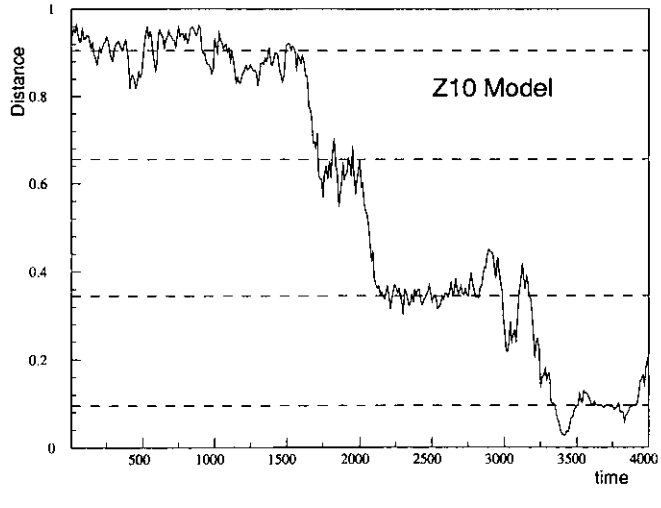

Figure 7. The time evolution of the distance between two configurations which are initially fully polarized in opposite directions and at $T = 0.25$ and for $L = 20$. The dashed lines indicate the position of the different attractors $\langle D_k \rangle = \sin^2(k\pi/10)$.

which yields

$$\langle D_k \rangle = \sin^2(k\pi/10)\,.$$

In figure 8 we show the distribution of the distances at $t = 1000$ for a sample of 200 pairs of configurations at $T = 0.25$. The histogram is sharply peaked along the attractors $\langle D_k \rangle$, in agreement with behaviour seen in figure 7 and which can be interpreted in terms of a strongly fluctuating phase. Indeed, in the spin wave phase the correlation length is infinite and the magnetization fluctuates without limit. The

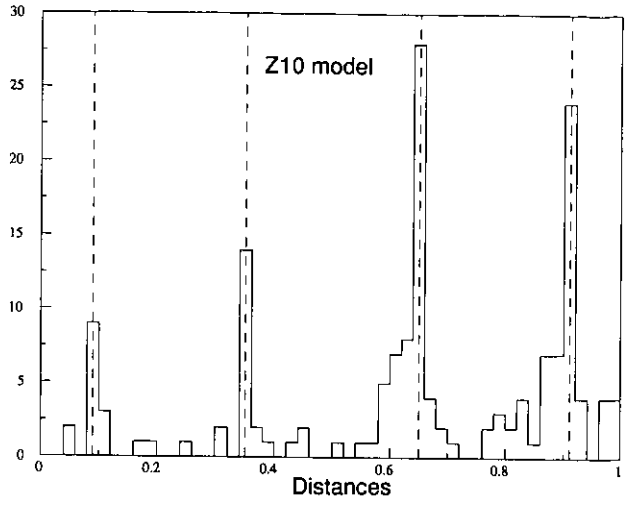

Figure 8. The distribution of distances at $t = 1000$ for the Z_{10} model on a 10×10 lattice at $T = 0.25$. The dashed lines indicate the position of the attractors.

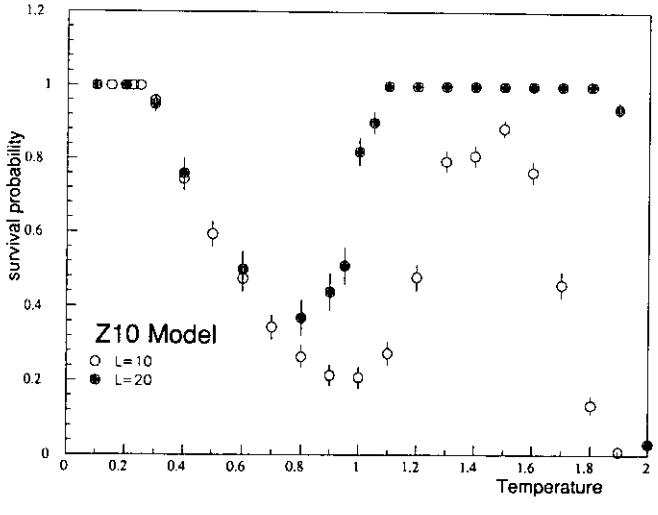

Figure 9. The survival probability at t_{max} as a function of the temperature for the Z_{10} model. The open circles correspond to $L = 10$ and $t_{max} = 1000$ whereas the full circles are for $L = 20$ and $t_{max} = 4000$.

dynamics revealed by the time evolution of the distance is consistent with such a behaviour of the system.

The dependence upon the initial conditions of the time evolution is another characteristic difference between the two phases. We have computed the averaged distance for initial configurations fully polarized with spins making the smallest possible angle $\theta = \frac{1}{5}\pi$ corresponding to $D(0) = 0.095$ (initialization 2). We observe in figure 5 the same change of regime as for initialization 1. Furthermore, there is a loss of initialization dependence for $T \geqslant 0.24$ which is in agreement with the above argument of large dynamical fluctuations. This result is somewhat different with that of [4] where the

spin wave phase is characterized by a strong dependence on initial conditions. Indeed, this discrepancy reflects the arbitrariness of the choice of the time cut-off t_{max}. As we take t_{max} longer than the characteristic relaxation time for the transition between two attractors, our distance is subjected to the fluctuations seen in figure 7 irrespective of the initial conditions. In [4], t_{max} being smaller than this relaxation time, the system appears to be blocked in the attractor selected by the initial conditions.

A second transition, which is less well-localized, occurs for $0.9 \leqslant T \leqslant 1.2$. Its presence is not visible in the variations of $\langle D \rangle$ and it manifest itself in figure 6 as a small drop in the behaviour of σ_D with the temperature. It is more clearly evident in figure 9, in the variation of the survival probability with T which slowly decreases as the temperature grows from $T = 0.24$ to $T \simeq 1.0$. A change of regime is marked by a sudden increase of $p_s(t_{max})$ which remains maximum for $1.0 \leqslant T \leqslant 2.0$. For $T \simeq 2.0$ an abrupt fall of $p_s(t_{max})$ down to zero, signals the transition to the high-temperature paramagnetic phase. In this intermediate region, between $T \simeq 1.0$ and $T \simeq 2.0$, the system evolves with small fluctuations, as in a ferromagnetic phase, but with no dependence on the initial conditions. This unexpected regime is similar to the one found in [4].

It may result from a partial breaking of the full Z_{10} symmetry into a Z_5 or Z_2 residual one. However, we shall see in the next section that a similar behaviour is observed for the Z_5 and the Z_7 models where such a mechanism is not allowed. In the next sections, we discuss the possible connection between this phase and some equilibrium property of the system. Alternatively, it could result from a pure dynamical effect as the analysis of Golinelli [6] may suggest.

To conclude this section, we stress that the method of distances leads to a clear identification of *four* different dynamic phases in the Z_{10} model, with three transition temperatures, $T_1 = 0.24$, $T_2 \simeq 1.05$ and $T_3 = 2.0$. The lowest and highest temperature phases correspond to the static ferromagnetic and paramagnetic ones, respectively. The first intermediate phase, for $T_1 \leqslant T \leqslant T_2$, is related to the expected spin wave phase, whereas the other intermediate phase for $T_2 \leqslant T \leqslant T_3$ has no known equilibrium equivalent. The transition temperature T_2, is difficult to locate precisely due to large finite-size effects, but our rough determination is compatible with the static value found in ref [14] $T = 1.0$.

4. The models Z_p for $p = 5, 6, 7$

The full Z_5 symmetric model as well as its 'clock' restricted version, have been investigated using renormalization group methods [8], mean field approximations [9] and perturbative expansions [10]. All of these analyses confirm the emergence of a soft phase in a very narrow range of temperature, with a Kosterlitz–Thouless type transition.

We have performed the same analyses as in section 3 for the Z_5 model. The results are displayed in figures 10, 11 and 12, for the averaged distance, σ_D and $p_s(t_{max})$ respectively, and may have to be compared to their equivalent for the Z_4 model (figures 2 and 4) and for the Z_{10} model (figures 5, 6 and 9). The data are clearly incompatible with a unique classical second order transition at the self-dual temperature $T_C = 0.923$, as in the Z_4 model. Instead, we observe the same behaviour as in the Z_{10} case for all our results. We distinguish a first transition at $T_1 \simeq 0.8$, marked by the abrupt jump in σ_D, (figure 11), followed by a soft phase, clearly indentifiable by the persistently

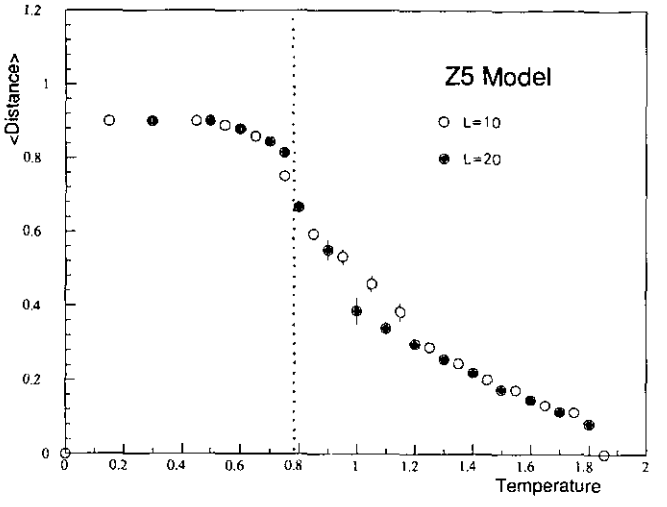

Figure 10. As figure 6, but for the Z_5 model.

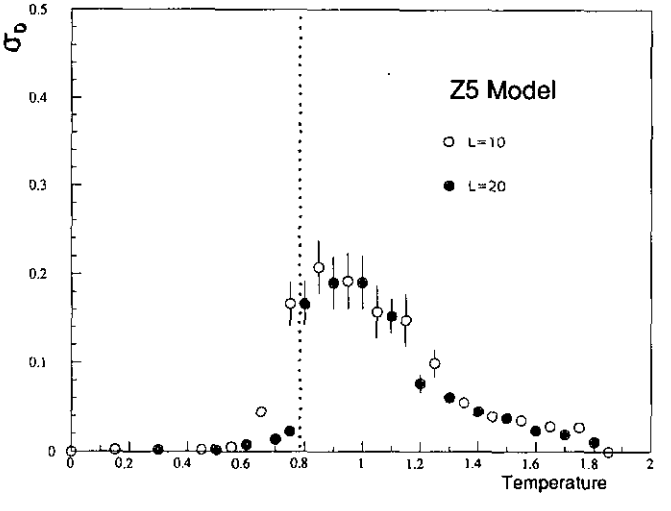

Figure 11. As figure 7, but for the Z_5 model.

large value of σ_D over a rather broad interval of temperature. The second transition is signalled by the sudden rise in the survival probability for $1.0 \leqslant T_2 \leqslant 1.2$, which remains maximum up to $T_3 \simeq 1.8$ where it falls to zero.

In conclusion, the dynamic phase diagram of the Z_5 model exhibits the same structure as in the Z_{10} case, with three transitions at $T_1 \simeq 0.8$, $1.0 \leqslant T_2 \leqslant 1.2$ and $T_3 \simeq 1.8$.

The first point concerns the clear evidence for the strongly fluctuating regime found between T_1 and T_2, which is presumably linked to the emergence of a spin-wave like phase, but in a range of temperature wider than expected in the static case [10].

The second point concerns the intermediate phase between T_2 and T_3, already observed in the Z_{10} and XY models, but not present in the Z_p models for $p \leqslant 4$. This

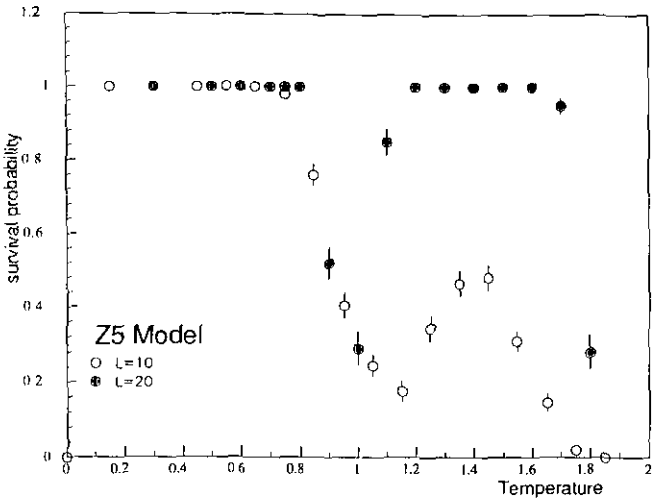

Figure 12. As figure 10, but for the Z_5 model.

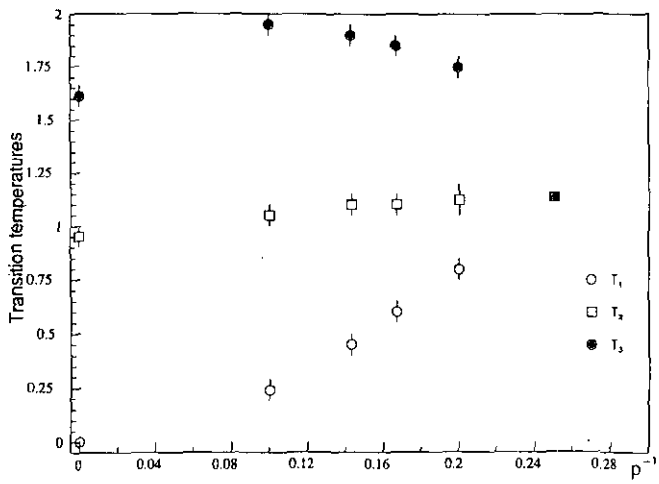

Figure 13. The dynamical transition temperatures of the Z_p models as a function of $1/p$ and the XY model ($p = \infty$) result of Golinelli and Derrida.

phase has no obviously known static equivalent, but since it occurs only in conjonction with the soft phase one could be tempted to connect the two transition points T_2 and T_3 within a same interpretation. The suggestion of Garel *et al* [15] of the existence of a disordered line crossing the paramagnetic phase is an appealing one and deserves further investigation.

We have reproduced the analysis for the Z_6 and the Z_7 models and found exactly the same dynamic phase diagram as in the Z_5 and Z_{10} cases. The transition temperatures are presented in figure 13 as a function of $1/p$ with the asymptotic value of the XY model obtained by Golinelli and Derrida [4]. The transitions at T_1 and T_3 are clearly marked and, being subject to small finite-size effects, their determination is rather precise. In contrast, an accurate measurement of T_2 is difficult due to the

essential point nature of the singularity, and one would need very large lattices and finite-size scaling analysis to get reliable and precise numbers [16]. Since our purpose is not a determination of the critical exponents, we only give a rough estimate of T_2.

We first observe in figure 13, that the transition temperature T_1 decreases as p grows, in conformity to what is expected for the associated static critical temperature, whereas the interval delimiting T_2, although quite stable, seems to slowly decrease and may reach, as $p \to \infty$, a value compatible with the measured dynamical critical temperature of the XY model $T_{KT} \simeq 0.95$ [4]. The upper transition temperature seems to extrapolate to a higher value than the XY one.

Duality arguments are used to relate the static critical temperatures T_1 and T_2 of the fully Z_p symmetric models [9,10], based on the Hamiltonian formulation, and of the generalized Villain model [8,17]. For this last model, one can derive the relation

$$T_1 T_2 = T_{SD}^2 \tag{8}$$

where $T_{SD} = 2\pi/p$ is the point where the model is symmetric under the duality transformation.

For the classical Z_p clock model the duality transformation generates additional couplings and it is no longer a symmetry of the Hamiltonian. Therefore there is no relation equivalent to (8). But for each value of p, one can find a temperature where these additional couplings are zero (exactly for Z_5) or small, making the model approximately self-dual. Let us call T_{SD} this temperature obtained by solving the duality equations of [9]. We find that the *dynamical* transition temperatures T_1 and T_2 and the self-dual one defined above, are in good agreement with a relation equivalent to equation 8, as for $p = 5, 6, 7, 10$ we obtain $T_{SD}^2/T_1 T_2 = 0.96, 0.95, 0.98, 1$, respectively. We interpret this phenomenological result as a confirmation of the link between the dynamic transition temperatures T_1 and T_2 and their equilibrium equivalent.

5. Conclusion

The heat bath dynamics of the Z_p symmetric clock models has been studied for $p = 4$, 5, 6, 7 and 10 by comparing the Monte-Carlo time evolution of two configurations, initially in different states, and evolving according to the same thermal noise.

The dynamic phase diagrams are quite different for $p = 4$ and for $p \geqslant 5$. In the first case, one observe two phases, which are identified as the ferromagnetic and paramagnetic equilibrium ones, with a transition temperature which coincides with the static one within the precision of the method. Although not presented here, we have obtained equivalent results for the Z_3 and Z_2 (Ising) models as a check of our method.

For $p \geqslant 5$, we find four different phases. Between the low-temperature ferromagnetic phase and the high-temperature paramagnetic one, a strongly fluctuating phase occurs, related to the soft spin-wave equilibrium one, together with a new unexpected phase, similar to the one found in the XY model [4]. It is characterized by a very sharply peaked distribution of distances, small fluctuations in the time evolution, and an averaged distance which decreases roughly linearly, independent of the initial conditions.

As this phase only appears, in the sequence of the Z_p models, in conjunction with the soft phase, one may think of an interpretation in terms of some equilibrium state of the gas of vortices. This has been suggested by Garel *et al* [15] for the XY model.

However, a similar effect appears in very different systems like the spin glasses [2], or in a dilute ferromagnetic model [6], where it has been exactly shown to have a purely dynamical origin. Moreover, in a recent study of the XY model based on a dynamics which preserves the O(2) invariance [18], this phase is not observed. All these results suggest interpreting this phase as a dynamical one, but its real nature is still far from clear and deserves further study.

The method of distances has given a qualitatively good insight into the dynamics of the clock model, but accurate quantitive results are not easy to obtain, mainly due to the large fluctuations and finite-size effects inherent to the Kosterlitz–Thouless transition. However, our results for the transition temperatures are in agreement with a phenomenological duality-like relation inspired from the generalized Villain model. This support the connection between the dynamic transitions and the equilibrium ones.

Finally we notice that the soft phase is clearly observable in the clock Z_5 model, unlike the general Z_5 symmetric one where it appears as a small effect [10]. We conclude that the distance method is very sensitive to the phase changes and may be a fruitful technique for exploring unknown phase diagrams.

Acknowledgments

We thank B Derrida and O Golinelli for helpful discussions.

References

[1] Binder K 1979 *Monte Carlo Methods in Statistical Physics* ed K Binder (Berlin: Springer)
[2] Derrida B and Weisbuch G 1987 *Europhys. Lett.* **4** 657
[3] Neumann A U and Derrida B 1988 *J. Physique* **49** 1647
[4] Golinelli O and Derrida B 1989 *J. Phys. A: Math. Gen.* **22** L939
[5] Stanley H E, Stauffer D, Kertsz J and Herrmann H 1987 *Phys. Rev. Lett.* **59** 2326
Herrmann H 1990 *Proc. Third Bar-Ilan Conf. on Frontiers in Condensed Matter Physics, Physica* **168A** and references therein
[6] Golinelli O 1990 *Preprint* CEN Saclay SPhT/90-034
[7] Wu F Y 1982 *Rev. Mod. Phys.* **54** 235
[8] Elitzur S, Pearson R B and Shigemitsu J 1979 *Phys. Rev.* D **19** 3698
[9] Alcarraz F C and Koberlee R 1981 *J. Phys. A: Math. Gen.* **14** 1169
[10] Bonnier B, Hontebeyrie M and Meyers C 1989 *Phys. Rev.* B **39** 4079
Bonnier B and Rouidi K 1990 *Phys. Rev.* B **42** 8157
[11] Aizenman M and Simon B 1980 *Phys. Lett.* **76A** 281
[12] Tang S and Landau D P 1987 *Phys. Rev.* B **36** 567
[13] Fröhlich J and Spencer T 1981 *Commun. Math. Phys.* **81** 527
[14] Seiler E, Stamatescu I O, Patrascioiu A and Linke V 1988 *Nucl. Phys.* B **305** 623
[15] Garel T, Niel J C and Orland H 1990 *Europhys. Lett.* **11** 349
[16] Gupta R, DeLapp J, Batrouni G G, Fox G C, Baillie C F and Apostolakis J 1988 *Phys. Rev. Lett.* **61** 1996
Ewards R G, Goodman J and Sokal A D 1990 *Preprint* Florida State University FSU-SCRI-90-99
Wolff U 1989 *Nucl. Phys.* B **322** 759
[17] Jos J V, Kadanoff L P, Kirkpatrick S and Nelson D 1977 *Phys. Rev.* B **16** 1217
[18] Chiu J and Teitel S 1990 *J. Phys. A: Math. Gen.* **23** L891